Continental Shelf Research 28 (2008) 1556–1567

Contents lists available at ScienceDirect

Continental Shelf Research

journal homepage: www.elsevier.com/locate/csr

Space–time variability of the Plata plume inferred from ocean color

Alberto R. Piola [a,b,*,1], Silvia I. Romero [a,b,2], Uriel Zajaczkovski [a,b]

[a] Departamento Oceanografía, Servicio de Hidrografía Naval, Buenos Aires, Argentina
[b] Departamento de Ciencias de la Atmósfera y los Océanos, Buenos Aires, Argentina

ARTICLE INFO

Article history:
Received 13 June 2006
Received in revised form
25 October 2006
Accepted 2 February 2007
Available online 26 March 2008

Keywords:
Ocean color
River plumes
Rio de la Plata
SeaWiFS
Estuary–shelf interactions
Interannual variability

ABSTRACT

Satellite ocean color and surface salinity data are used to characterize the space–time variability of the Río de la Plata plume. River outflow and satellite wind data are also used to assess their combined effect on the plume spreading over the Southwestern South Atlantic continental shelf. Over the continental shelf satellite-derived surface chlorophyll-*a* (CSAT) estimated by the OC4v4 SeaWiFS retrieval algorithm is a good indicator of surface salinity. The log(CSAT) distribution over the shelf presents three distinct modes, each associated to: Subantarctic Shelf Water, Subtropical Shelf Water and Plata Plume water. The log(CSAT) 0.4–0.8 range is associated with a sharp surface salinity transition across the offshore edge of the Plata plume from 28.5 to 32.5. Waters of surface salinity <31, derived from mixtures of Plata waters with continental shelf waters, are associated to log(CSAT) >0.5. In austral winter CSAT maxima extend northeastward from the Plata estuary beyond 30°S. In summer the high CSAT waters along the southern Brazil shelf retreat to 32°S and extend south of the estuary to about 37.5°S, only exceeding this latitude during extraordinary events. The seasonal CSAT variations northeast of the estuary are primarily controlled by reversals of the along-shore wind stress and surface currents. Along-shore wind stress and CSAT variations in the inner and mid-shelves are in phase north of the estuary and 180° out of phase south of the estuary. At interannual time scales northernmost Plata plume penetrations in winter (~1200 km from the estuary) are associated with more intense and persistent northeastward wind stress, which in the period 2000–2003, prevailed over the shelf south of 26°S. In contrast, in winter 1999, 2004 and 2005, characterized by weaker northeastward wind stress, the plume only reached between 650 and 900 km. Intense southwestward plume extensions beyond 38°S are dominated by interannual time scales and appear to be related to the magnitude of the river outflow. The plume response to large river outflow fluctuations observed at interannual time scales is moderate, except offshore from the estuary mouth, where outflow variations lead CSAT variations by about 2 months.

1. Introduction

Continental runoff discharges freshwater, sediments, organic material and dissolved substances onto the continental shelf producing a significant impact on the ocean's physical, chemical and biological properties. The Río de la Plata (Plata hereafter) drains nearly 20% of the surface area of South America and discharges about 23,000 $m^3 s^{-1}$ of freshwater on the western South Atlantic shelf at 35°S. The estuarine front is characterized by vertical nutrient fluxes, which produce fertilization and high chlorophyll-*a* (chl-*a*) concentrations near the estuary (Carreto et al., 1986), creating a nursery for coastal species (Acha et al., this issue). Several hundred kilometers northeast from the estuary the low salinity coastal waters derived from the Plata are also associated with high nutrient and chl-*a* concentrations, phytoplankton (Ciotti et al., 1995), benthic foraminifera (Eichler et al., this issue) and commercially important species (Muelbert and Sinque, 1996; Sunyé and Servain, 1998). Hydrographic, satellite and biological data collected over the shelf suggest that at times the Plata influence may extend northeastward beyond 1000 km from the estuary (e.g. Emilson, 1961; Campos et al., 1999) and may explain the observation of subantarctic species as far north as 22°S (Stevenson et al., 1998).

Changes from lower river outflow, and on-shore and upwelling winds in austral spring–summer to larger outflow, and offshore and downwelling winds in fall–winter, alter the upper layer salinity distribution within the estuary (Guerrero et al., 1997; Framiñan et al., 1999). Historical hydrographic data reveal that the meridional extension of the Plata plume undergoes large amplitude seasonal fluctuations. Based on the surface salinity distribution the Plata waters extend northeastward beyond 26°S in austral fall–winter and retract to about 33°S in spring–summer

* Corresponding author at: Departamento Oceanografía, Servicio de Hidrografía Naval, Av. Montes de Oca 2124, C1270 ABV, Buenos Aires, Argentina.
E-mail address: apiola@hidro.gov.ar (A.R. Piola).
[1] Also at CONICET, Argentina.
[2] Also at ESCM-INUN, Instituto Universitario Naval, Buenos Aires, Argentina.

0278-4343/$ - see front matter © 2008 Elsevier Ltd. All rights reserved.
doi:10.1016/j.csr.2007.02.013

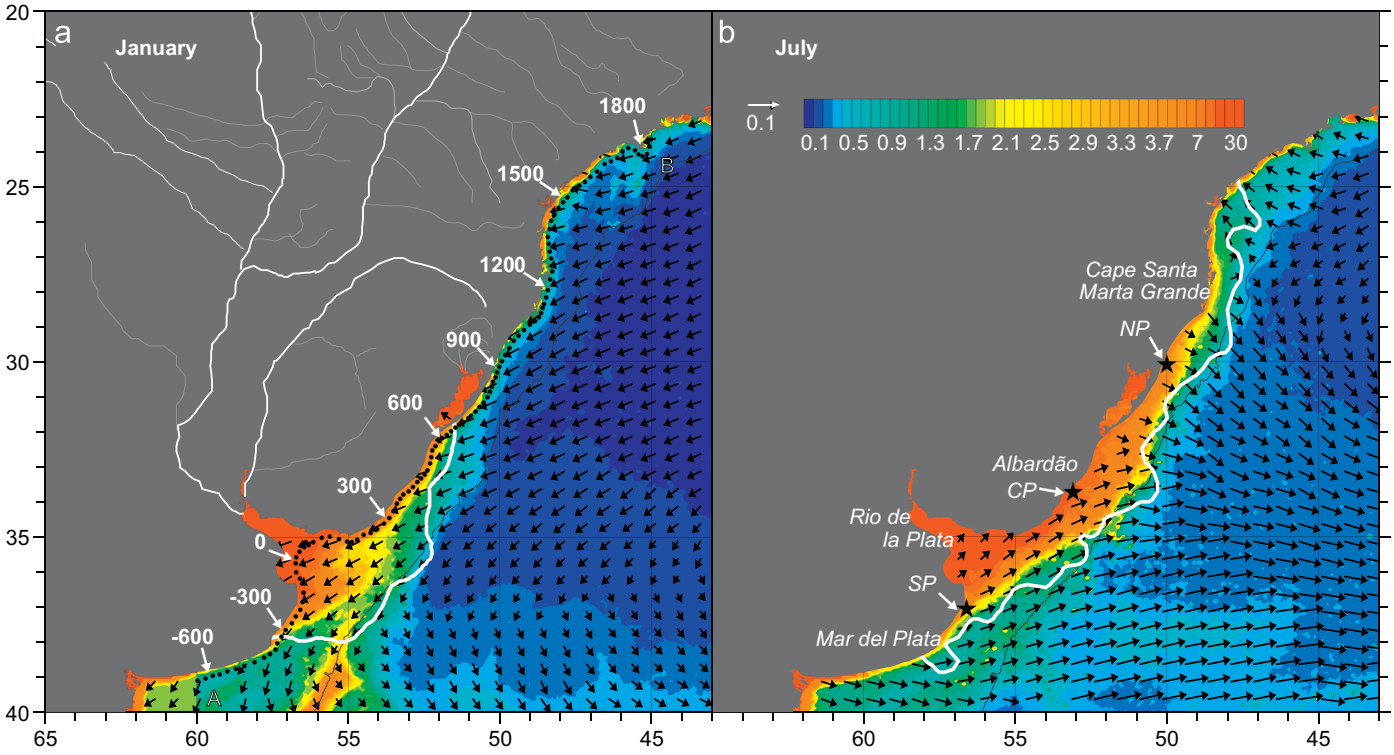

Fig. 1. January (a) and July (b) climatological CSAT (mg m^{-3}) distributions derived from monthly mean SeaWiFS images of 9 km spatial resolution (1998–2005). Also shown are climatological wind stress fields derived from monthly mean QuikSCAT winds from July 1999 to December 2005. The black dotted line in (a) shows the location of along-shore section AB (see Fig. 6a and b), also shown are distances to estuary (in km) along this line and the major Plata tributaries. SP, CP and NP shown in (b) are the locations selected to depict the seasonal and interannual variations of CSAT and wind stress. The white line in each plot is the climatological position of the 33.5 isohaline derived from historical hydrographic data.

(Fig. 1, Piola et al., 2000). At 30°S the seasonal variability in the distribution of the Plata plume causes large temperature (~3 °C, Campos et al., 1999) and salinity fluctuations (~4, Piola et al., 2005). The seasonal fluctuations of the Plata plume were recently confirmed by high-resolution synoptic surveys carried out over the shelf and slope in 2003 and 2004. In winter 2003, mixtures of about 5% of Plata waters were observed 1200 km (~28°S) from the estuary, while in summer 2004 the 5% mixture retracted to 330 km from the estuary (34°S) and expanded offshore beyond the shelf break (Möller et al, this issue).

Historical data, together with reanalysis wind stress data and numerical simulations suggest that changes in the along-shore wind stress are the main factor affecting the distribution of low salinity waters over the shelf (Piola et al., 2005). Numerical simulations of the Plata plume suggest that near the estuary wind forcing is mostly important during the summer, when prevailing easterlies force low salinity waters southward, while in winter the northeastward plume development is due to the combined effect of river discharge and the Coriolis force (Simionato et al., 2001; Huret et al., 2005). Other simulations of the Plata plume (Pimenta et al., 2005) and simplified models (Palma and Sitz, 2005) explored the role of large-scale wind forcing over the entire shelf area, concluding that wind forcing plays a central role in determining the along-shore plume extent.

There is strong evidence that large precipitation anomalies over central South America, associated with El Niño (EN, Ropelewski and Halpert, 1987; Kiladis and Diaz, 1989) events, significantly increase the discharge of the major Plata tributaries (Depetris et al., 1996; Mechoso and Perez Iribarren, 1992). Consequently, the Plata outflow presents large interannual variability, with maxima beyond 80,000 m^3 s^{-1}, and minima of about 11,000 m^3 s^{-1}. Theoretical arguments and numerical experiments indicate that high river discharges should lead to increased plume penetrations (Kourafalou et al., 1996; Garvine, 1999). However, surface salinity observations from the southern Brazil continental shelf suggest that the large discharge events do not lead to stronger northeastward plume penetrations (Piola et al., 2005). The apparent decoupling of the northeastward plume penetration from the river discharge is explained by anomalous northeasterly winds frequently prevailing during EN episodes, which effectively oppose to the northward spreading of low salinity waters (Piola et al., 2005).

Continental runoff introduces suspended material and yellow substances (colored dissolved organic matter), which alter the optical properties of the coastal ocean (e.g. Binding and Bowers, 2003). These substances enhance the upward water-leaving radiance and lead to an overestimation of continental shelf satellite-derived surface chl-*a* (CSAT) in coastal waters by standard retrieval algorithms (IOCC, 2000; Hu et al., 2000). Consequently, chl-*a* in the Plata influenced region is highly overestimated by satellite color measurements (Armstrong et al., 2004; Garcia et al., 2005, 2006). Based on CSAT distributions the area influenced by the Plata discharge has been identified as a distinct biogeographical region characterized by high surface reflectance (Gonzalez-Silvera et al., 2004). Therefore, a relation between salinity and CSAT may be expected in near coastal waters influenced by the river outflow. A preliminary analysis of CSAT vs. surface salinity based on historical data showed that near 30°S, where there are large seasonal salinity variations on the continental shelf, sea surface salinity monthly minima are linearly correlated with CSAT ($r^2 = 0.78$, Piola and Romero, 2004).

Though the Plata outflow and the variability of the distribution of low salinity waters produce a strong impact on the near-shore ecosystem, there is limited understanding of their variations from

intraseasonal to interannual time scales. In this study we take advantage of the facts that the river outflow enhances the chl-*a* concentration and that as it discharges suspended matter and yellow substances, it further alters the optical properties of the neighboring ocean. Our working hypothesis is that through these combined effects river runoff regionally enhances the satellite retrieved chlorophyll concentration, thus providing a more effective tracer of the river-derived low salinity waters than other indicators which only capture some of the discharge impacts, like yellow substances (see Binding and Bowers, 2003) or suspended matter. We use CSAT as a tracer of Plata influenced waters to analyze the space–time variability of the river plume during the period 1998–2005. The approach is similar to that of Piola and Romero (2004) and Gonzalez-Silvera et al. (2006); however, satellite data here combined with high-resolution *in-situ* surface salinity data collected in austral winter 2003 and summer 2004. Our primary aim is to assess the response of the river plume along-shore extent to changes in the magnitude of the river discharge and the intensity and direction of the wind stress. In Section 2 we describe the data and methods. *In-situ* surface salinity is compared with concomitant satellite measurements in Section 3, showing that CSAT is a good indicator of low salinity waters derived from the Plata. Seasonal and interannual variations of the Plata plume, as revealed by satellite data for the period 1998–2005 are presented in Section 4. In Section 5 the results are discussed and compared with previous studies of the Plata plume variability. Finally, conclusions are presented in Section 6.

2. Data and methods

We use daily high-resolution CSAT data collected by the Sea-viewing Wide Field-of-view Sensor (SeaWiFS) at 1 km resolution and estimated by the OC4v.4 algorithm after NASA's fourth reprocessing. The data were processed using all quality control flags and masks routinely applied to Level 2 ocean color processing (see Patt et al., 2003). In addition, a CSAT time series on an along-shore section located about 20 km from shore (AB in Fig. 1a) was constructed using SeaWiFS Level-3 monthly data of 9 km resolution from January 1998 to December 2005. The section spans from 39°S to 23°30′S, in the South Brazil Bight. To further evaluate the distribution of Plata-derived waters, we analyzed the cross-shelf structure of the attenuation coefficient at 490 nm (K490) at 1 km resolution. K490 is an indicator of light penetration in the water column in the green and blue parts of the spectrum.

Monthly Plata outflow data estimated at the river mouth in the period 1931–2005 is from Borús et al. (2006) and satellite monthly mean wind stress data from July 1999 to December 2005 from the QuikScat scatterometer. QuikScat winds at 25 km resolution are available from remote sensing systems (www.remss.com). To complete the wind stress time series during the CSAT period from January 1998 to June 1999, prior to the availability of QuikSCAT data, we use the 1° resolution ERS-2 data made available by IFREMER (www.ifremer.fr/cersat). For the present analysis wind stress is decomposed in along-shore (τ_y) and cross-shore components (τ_x). Table 1 indicates the directions for decomposition of the wind stress along different coastal sections.

In-situ surface salinity, used to establish the relation with CSAT, is from the Nicop-Laplata cruises, collected in late Austral winter from 20 August to 2 September 2003 and in mid-summer from 1 to 19 February 2004. Near-surface salinities (~3 m depth) were measured using SeaBird Electronics Seacat 21 thermosalinographs, calibrated to within 0.05 based on CTD data and water samples. The winter and summer *in-situ* data were collected at 20 and 10 s sampling rates, respectively. Availability of ocean color data is strongly limited by cloud cover. For comparison, only *in-situ* surface salinity observations collected within 12 h and 3 km of valid CSAT data were used for the analysis. As the CSAT spatial resolution of 1 km is low compared to the shipborne surface salinities, even when collected at the highest sailing speeds of around 12 knots, we averaged all surface salinity observations collected within 5 min time intervals. For the analysis of along-shore CSAT and wind stress variability the data were spatially smoothed with a running mean, eliminating features of less than ~70 km in the along-shore direction, which are not relevant in the context of this work.

Table 1
Orientations selected for wind decomposition in along-shore and cross-shore directions

Section	Latitude °S	Along-shore °True	Cross-shore °True
South	39–38	065	155
Central	38–28	035	125
South Brazil Bight (S)	28–25.5	000	090
South Brazil Bight (N)	25.5–23	045	135

3. Sea surface salinity vs. CSAT

The relation between sea surface salinity (S) and CSAT is illustrated by the cross-shelf section collected off Albardão (~33°S) between 12:40 GMT 26 August and 10:46 GMT 27 August 2003 (Fig. 2). The section spans the transition from high CSAT–low salinity Plata plume waters to low CSAT–high salinity shelf and open ocean waters in the southern Brazil continental shelf. The data are plotted as a function of distance from shore. CSAT data used to construct Fig. 2 is from a 1 km resolution SeaWiFS image collected on 27 August 2003 between 15:21 and 15:32 GMT. *In-situ* data collected earlier than 12 h before the satellite path are dashed in Fig. 2. In the inner shelf (up to 60 km from shore) surface salinities lower than 28.5 are associated with Plata plume waters. A sharp increase, to S~32.5, observed 80 km from shore marks the offshore plume front and the transition to Subantarctic Shelf Waters. At the inshore low salinity band, extending about 60 km from shore, CSAT is higher than 5 mg m^{-3}, and decreases to <2.5 mg m^{-3} about 90 km from shore. This sharp CSAT transition is observed close to the location of the S front. Due to cloud cover in the southernmost region, there are fewer observations within the outer estuary than along the northeastward extension of low salinity water. The summer observations off the Plata estuary, when low salinity waters extend primarily offshore, indicate that though CSAT is high, at salinities lower than ~27 the CSAT–salinity relation is not as well defined as across the plume further north. The mean S calculated over 0.1 log (CSAT) class intervals for data collected in August 2003 and February 2004 throughout the area covered by the *in-situ* surveys is shown in Fig. 3. Based on the observed salinity distribution as a function of CSAT there are three distinct water masses: Subtropical (S~36), Subantarctic Shelf Water ($32<S<34$) and Plata plume water ($S<31$). Moreover, each water mass is associated with a distinct mode in log(CSAT) relative abundance. The sharp salinity transition from $S>32.5$ to $S<28$ observed across the Plata plume front is closely associated with log(CSAT) within the 0.4–0.8 range, or CSAT ~2.5–6 mg m^{-3}. Because of the southwestward retraction of the Plata plume during summer and due to intense cloud cover during the occupation of the southernmost hydrographic sections in early February 2004 very few low S–high CSAT observations are available in summer. The S–log(CSAT) correlation coefficient in winter is 0.95 and decreases to 0.84 in summer.

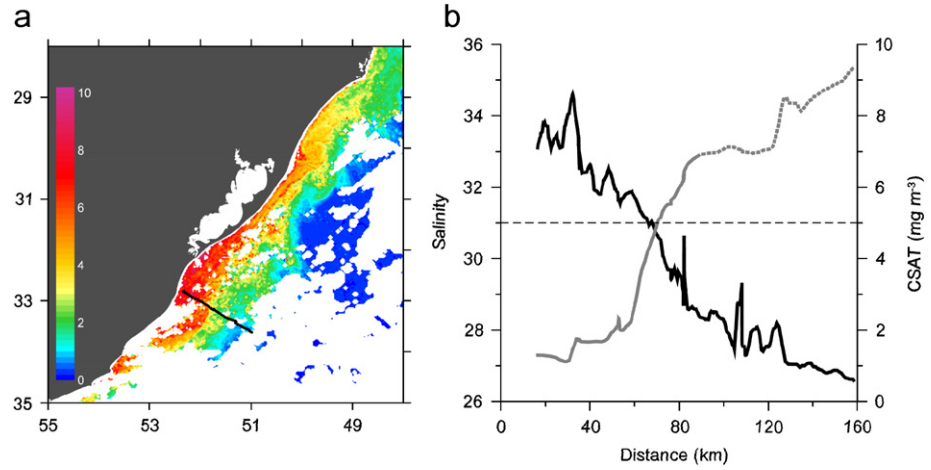

Fig. 2. (a) High-resolution (1 km) CSAT distribution (mg m^{-3}) derived from a SeaWiFS path collected on 27 August 2003 between 15:21 and 15:32 GMT. The black line indicates the cruise track shown in (b). (b) Cross-shelf surface salinity (gray) observed by the shipborne thermosalinograph and CSAT (mg m^{-3}) retrieved from the image shown in a. The dotted line in surface salinity indicates data gathered more than 12 h before the satellite path and the dashed line marks CSAT = 5 mg m^{-3}, associated with the plume front.

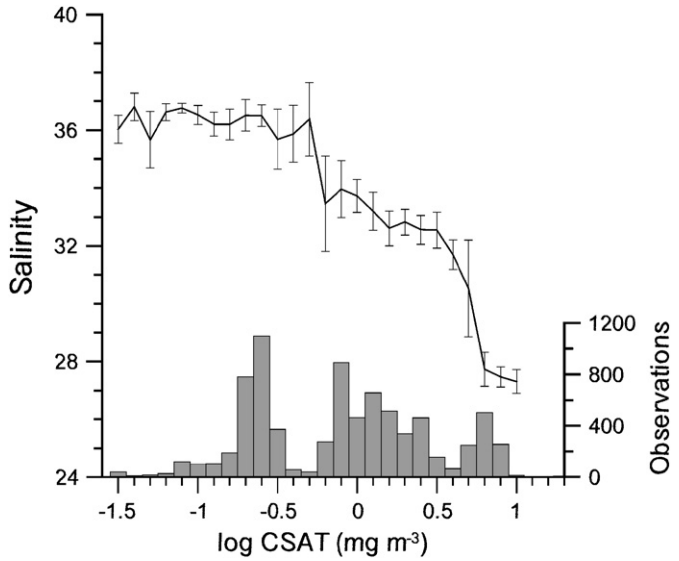

Fig. 3. Mean surface salinity calculated over 0.1 log (CSAT) class intervals using all concomitant *in situ* and satellite data. The vertical error bars in salinity are the standard deviations around the mean. Also shown along the *x*-axis is a histogram of relative abundance of satellite samples within each class interval.

To asses the relation between turbid waters and surface salinity we tested the K490 vs. salinity relation and found that though qualitatively the K490 cross-shelf structure (not shown) is similar to that of CSAT, its distribution is noisier and the gradients across the plume's edge are not as well defined as the CSAT gradients. Consequently, the *S*–CSAT correlation coefficient across the offshore edge of the Plata plume off Albardão, between 60 and 85 km from shore (−0.76), is significantly higher than the *S*–K490 (−0.35), suggesting that CSAT is a better proxy of the low salinity waters. Since northward flowing Subantarctic Shelf Water presents a tight salinity within the 33.6–33.8 range, all waters fresher than ~33.5 must have a Plata contribution (Piola et al., 2000). Thus, the 33.5 isohaline is frequently taken as the offshore edge of waters influenced by the Plata outflow (Fig. 1, Piola et al., 2000). The correspondence between the mean January and July CSAT distributions for the period 1998–2005 and the historical summer and winter locations of Plata influenced waters as determined by the 33.5 isohaline suggests that the CSAT–*S* relation derived from the synoptic salinity distributions may be valid at longer time scales. Given the high correlation between concomitant *S* and CSAT data, in the following sections we use monthly averaged CSAT data to further investigate the variability of Plata plume waters.

4. Results

4.1. Seasonal variability

To investigate the seasonal variability of the Plata plume and its relation to river outflow and along-shore winds we selected three inner shelf sites located near 37°S (SP), 34°38′S (CP) and 30°53′S (NP, see Fig. 1b). CP and NP are located north of the estuary and SP south of the estuary. Monthly means are calculated based on the 1998–2005 monthly time series of each variable. At CP and NP CSAT presents a well-defined seasonal cycle, with maxima in July and minima from October through March (Fig. 4). In contrast, at SP the highest CSAT values (~7 mg m^{-3}) occur in austral summer, and the lowest values (~5 mg m^{-3}) are observed from May through September. Though SP is closest to the estuary, the CSAT maximum is significantly lower that at CP (> 10 mg m^{-3}). Also, note that the seasonal CSAT fluctuations at SP present smaller amplitude than at CP and NP (Fig. 4a–c). As it will be discussed later, the CSAT fluctuations north and south of the estuary are quite distinct because southwestward plume penetrations are small compared to northeastward penetrations. The seasonal CSAT fluctuations are in agreement with the mean January and July distributions shown in Fig. 1. At SP and CP the along-shore wind stress reverses from negative (southwestward) between October and March, to positive (northeastward) from April to September (Fig. 4a and b). The along-shore wind stress at NP presents a similar structure, but southwestward wind stress dominates throughout the year. However, the relatively large wind stress standard deviation observed at NP suggests substantial interannual variability, including wind reversals, in the northern shelf during winter (Fig. 4c). While at CP and NP, located north of the estuary, CSAT varies in phase with τ_y, at SP, located southwest of the estuary, the seasonal variations of wind stress and CSAT are 180° out of phase. The Plata outflow presents only moderate seasonal variations, with relative maxima in May and

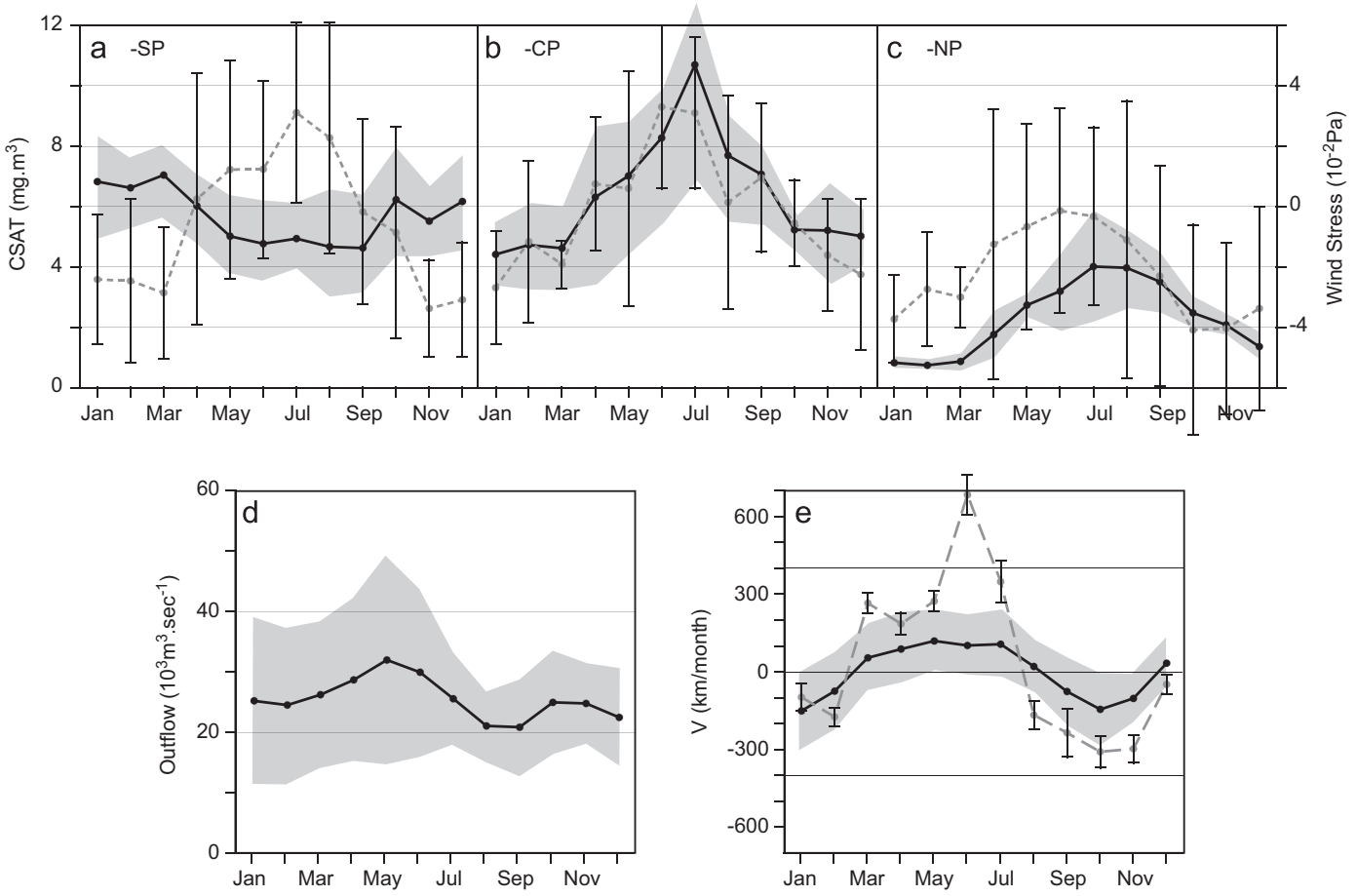

Fig. 4. Monthly mean time series (1998–2005) of CSAT (black, in mg m^{-3}) and along-shore wind stress (gray dashed line, in 10^{-2} Pa) at SP (a), CP (b) and NP (c). Standard deviations are shown in gray shading for CSAT, and by vertical lines for wind stress. The locations of SP, CP and NP are indicated in Fig. 1b. (d) The Río de la Plata outflow ($m^3 s^{-1}$, standard deviations in gray shading). (e) CSAT along-shore spreading velocity (V_{CSAT} in km/month, black dots and line, standard deviations in gray shading) and drifter derived along-shore surface velocity (km/month, gray dashed line), standard deviations shown by vertical lines.

October–November, but the standard deviations around the monthly means are large, suggesting interannual variations of relatively large amplitude (Fig. 4d).

Based on the northernmost monthly location of the 0.5 log (CSAT) isopleth we estimated the rate of advance of the Plata plume, which we refer to as V_{CSAT}. The record-length monthly mean speeds present two well-defined periods, with positive (northeastward) velocities from March through August and negative (southwestward) velocities from September through February (Fig. 4e). V_{CSAT} is anomalous (positive) in December, when a southwestward retraction might be expected. This is primarily due to the large positive (northeastward) velocity observed in December 1999 (245 km/month = 0.09 m s^{-1}, see Fig. 6a), but in December 1998, 2003 and 2004 small positive values are also observed. This suggests that the plume behavior is more variable in December. V_{CSAT} is uniform, about 100 km/month (0.04 m s^{-1}) during the positive phase and peaks at −150 km/month (−0.06 m s^{-1}) during the southwestward retraction phase in October.

4.2. Interannual variability

Interannual variability of the Plata plume is described based on time series of monthly mean CSAT at the selected locations (Fig. 5) and a space–time plot of log (CSAT) along the near-shore section AB (see Fig. 1a). The CSAT monthly time series, smoothed with a 3-month running mean, reveal marked interannual variability, with largest amplitudes in 2001 and 2002 (Fig. 5a). As suggested by the record-length monthly mean variations (Fig. 4), CSAT variations at SP are out of phase with CSAT at CP and NP, with maxima in austral summer and minima in winter (Fig. 5a). The along-shore wind stress at SP and CP reverses seasonally throughout the record length and presents a relatively large amplitude in the period 2000–2003 (Fig. 5b). However, the northeastward wind stress at CP was weak and of short duration in the austral winters of 1998, 1999 and 2004. In addition southwestward wind stress at NP is more intense than at SP and CP, with peaks observed in late spring. Most of the time the wind stress varies in phase, except at NP during winter and spring of 2004. The Plata presented a large outflow (>70,000 $m^3 s^{-1}$) in mid 1998, associated with EN (Fig. 5c). The relatively high CSAT values observed in winter of 1998 at CP and SP are probably related to the high Plata outflow at that time. After early 1999 the Plata outflow oscillated between ~20,000 and 30,000 $m^3 s^{-1}$, only exceeding 30,000 $m^3 s^{-1}$ between mid-2002 and early 2003.

Section AB is ~2500 km long running from 39°S, through the outer Plata estuary to 23°30′S, in the South Brazil Bight, and spans the region of largest CSAT seasonal variability. The CSAT and along-shore wind stress distributions along line AB are presented in along-shore coordinates with origin in the Plata outer estuary, negative southward and positive northward. CSAT presents the well-defined seasonal pattern associated with northeastward penetrations of high CSAT–low salinity water in austral winter,

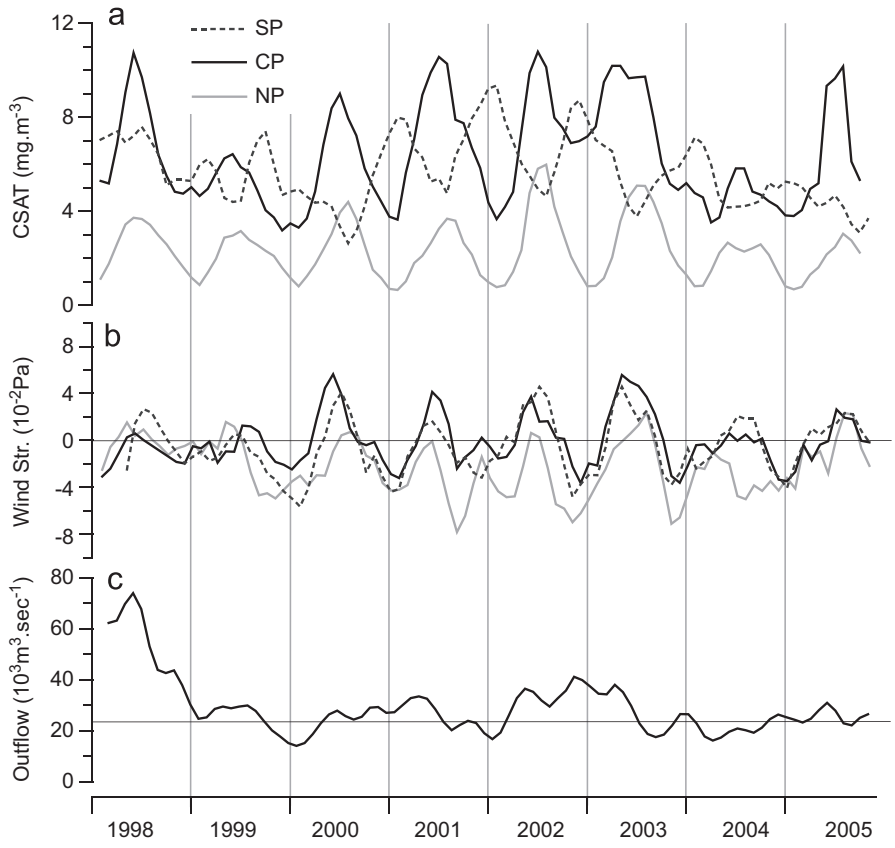

Fig. 5. Monthly time series (1998–2005) of (a) CSAT (in mg m^{-3}) at SP (dashed gray), CP (solid black) and NP (solid gray), (b) along-shore wind stress (in 10^{-2} Pa) at SP (gray dashed), CP (solid black) and NP (solid gray) and (c) Plata outflow (in 10^3 m^3 s^{-1}). The locations of SP, CP and NP are indicated in Fig. 1b. The mean river outflow is indicated in (c).

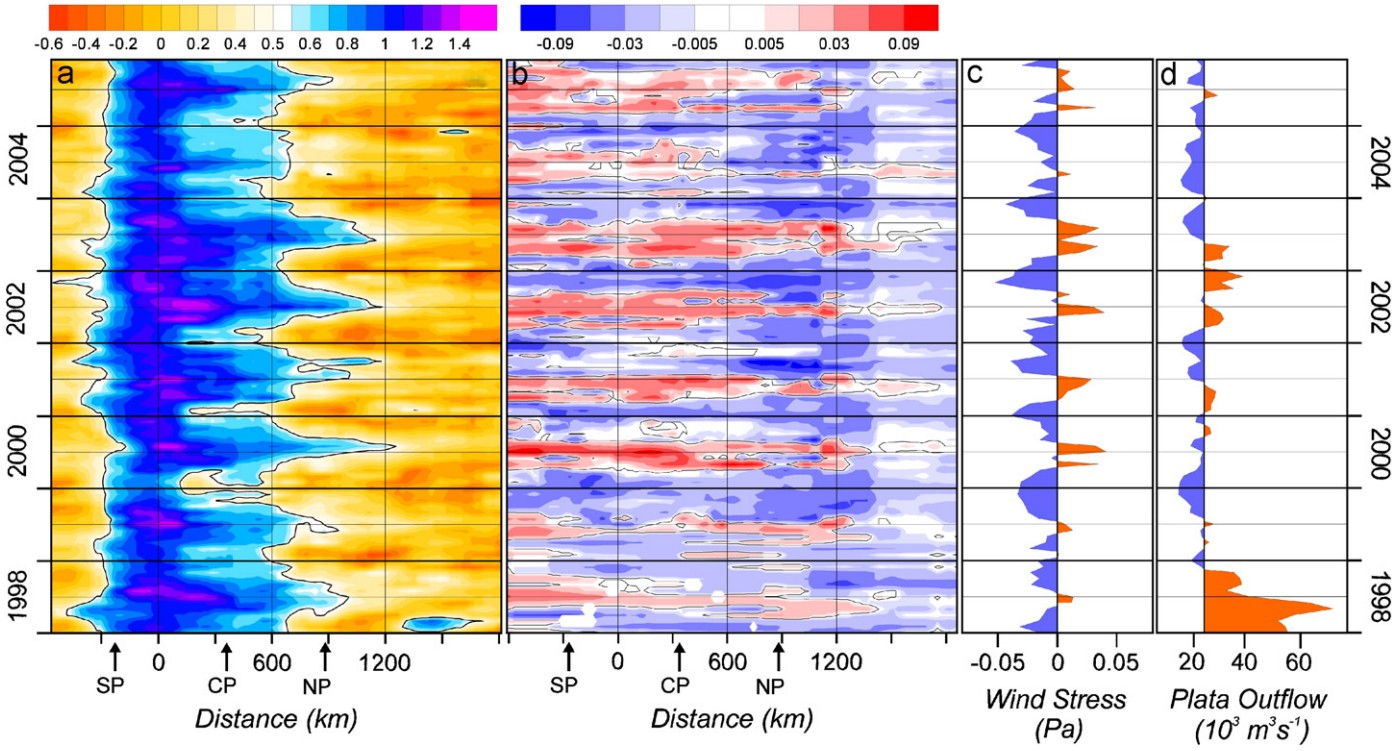

Fig. 6. (a) Space–time plot of monthly log (CSAT (mg m^{-3})) along section AB for the period 1998–2005 (for location see Fig. 1a). The contour is 0.5, associated with CSAT ~3 mg m^{-3}, (b) as in (a) for along-shore wind stress (Pa), (c) along-shore averaged monthly wind stress (Pa) and (d) monthly Plata outflow (10^3 m^3 s^{-1}). The zero wind stress and mean Plata outflow (23,000 m^3 s^{-1}) lines are indicated in (c) and (d), respectively. Above (below) average wind stresses and outflows in (c) and (d) are shown in red (blue).

and retractions in summer (Fig. 6a). The CSAT seasonal fluctuations are more intense from the estuary to about 1200 km (28°S). The structure of the log (CSAT) variations is virtually identical to the CSAT pattern (not shown). Based on the analysis of concomitant log (CSAT) and S observations (Fig. 3), the along shelf penetration of low salinity waters, is associated with log (CSAT) >0.5 (CSAT $>3\,\mathrm{mg\,m^{-3}}$). Also shown in Fig. 6 are the space–time plot and along shelf mean of τ_y and the Plata outflow. Changes in coast orientation (see Table 1) cause the marked changes in τ_y magnitude observed at about 1400 km (Fig. 6b). τ_y presents a stronger seasonal cycle in the southern region, up to 700 km from the estuary (see also Figs. 4a–c). In April 1998 the Plata outflow exceeded $70{,}000\,\mathrm{m^3\,s^{-1}}$ and in July the river plume, as indicated by the 0.5 log (CSAT) isopleth, extended 900 km northeast of the estuary, following a period when the wind stress was 0.025 Pa. In contrast, in July–September 2003, with a river outflow of only about $15{,}000\,\mathrm{m^3\,s^{-1}}$ and a wind stress of 0.04 Pa, the plume reached ~1200 km (Fig. 6a). The southward retreats also appear to be closely related to variations in τ_y. In spring 2002, in response to a strong southwestward wind stress (−0.07 Pa), and though the river outflow exceeded $30{,}000\,\mathrm{m^3\,s^{-1}}$, the Plata plume retracted from >1200 to ~900 km from the estuary. The following summer, however, the plume presented the least southward retreat (~600 km), suggesting an outflow effect at that location. Near-shore plume penetrations south of the estuary are more limited than northward penetrations, reaching about 300–500 km. In addition to an intense penetration in austral fall 1998, possibly associated to the large Plata outflow, there is another event in late 2002, also following a period of above average river outflow (Fig. 6d). The period of least southward penetration, observed in mid-2000, appears to be associated with mean outflow and strong northeastward wind stress prevailing south of the estuary (Fig. 6b–d).

5. Discussion

5.1. Seasonal variability

Based on data collected in late August 2003 and February 2004 on the region of influence of the Rio de la Plata over the continental shelf we find a high correlation (~0.9) between concomitant S and log (CSAT) observations. Due to intensive cloud cover, the data are more representative of austral winter than summer conditions. Though these results are based on data collected on two synoptic surveys only, a preliminary analysis of historical hydrographic data also found that near 30°S CSAT monthly means and monthly S minima are significantly correlated (Piola and Romero, 2004). Our findings are confirmed using an independent data set collected across the Rio de la Plata outer estuary and adjacent shelf (see Armstrong et al., 2004). We reanalyzed their data and found that though CSAT grossly overestimates *in-situ* chl-*a* within the Plata estuary, OC2v2 retrieved CSAT across the plume edge is linearly correlated with surface salinity ($r^2 = 0.82$). The present analysis of CSAT data for the period 1998–2005 reveals northeastward plume penetrations extending beyond 30°30′S (850 km from the estuary) during late austral fall and early spring (May–September), and retractions to at least 33°S (500 km northeast of the estuary) in late spring to early fall (November–March, Fig. 6a). The CSAT variability in the region of influence of the Plata plume north of the estuary is dominated by the annual cycle (Garcia and Garcia, this issue). As noted above, in winter the northernmost plume penetration regions, illustrated by the variability at NP, present a large τ_y standard deviation. The large wind variability may explain the increased relative CSAT variations observed at that location in winter (Fig. 4c). Though in late spring wind variability at NP is still large, as the plume retreats south of this location, CSAT is relatively insensitive to these changes (Fig. 4c). Thus, the seasonal meridional plume migrations north of 33°S are mainly regulated by the seasonal variations of τ_y, in agreement with analyses based on historical wind and hydrographic data (Piola et al., 2005) and numerical simulations (Palma and Sitz, 2005; Pimenta et al., 2005). The winter northeastward penetrations of the plume are also associated with increased plume width at 34°S (Gonzalez-Silvera et al., 2006; Garcia and Garcia, this issue). The CSAT plume extent south of the estuary does not present such a strong seasonal cycle as it does to the north (Fig. 4a), the amplitude of the signal being $\sim 2\,\mathrm{mg\,m^{-3}}$, comparable with the standard deviations around the monthly means (Fig. 4a).

The vertical extent of the Plata-derived low salinity waters also presents substantial seasonal variations. Hydrographic data collected during the Nicop-Plata expeditions show that as the Plata plume expands offshore during summer it forms a shallow (~20 m) low salinity layer separated by a sharp halocline from a relatively saline lower layer (Möller et al., this issue; Piola et al., this issue). In contrast, during winter, when the plume extends northeastward along the inner and mid-shelves, it is vertically quasi-homogeneous and bottom trapped. In agreement with these results, volumetric T–S analyses suggest that the volume of Plata-derived water found over the shelf is larger during winter than summer (Möller et al., this issue).

As described above, the seasonal fluctuations of the Plata plume are primarily associated with northeasterly winds in summer, which oppose to the development of the coastal current and southwesterly winds in winter, which favor the along-shore plume growth (Fig. 1). Since periods of increased (decreased) CSAT observed along the inner shelf between 34°S and beyond 27°S are associated with downwelling (upwelling) winds, it is unlikely that the observed CSAT variations are due to a response to wind-induced changes in vertical nutrient fluxes, commonly referred to as coastal upwelling. Instead, it is suggested that the observed CSAT variations are associated with along shelf advection of low salinity waters derived from the Plata. Northeastward plume penetrations in winter (Fig. 6a, see also Gonzalez-Silvera et al., 2006), coincide with downwelling favorable winds (Figs. 5c and 6b). Though upwelling events during winter are possible, for instance associated to the passage of cold fronts, it is unlikely that such events will produce a significant phytoplankton bloom under winter conditions. In addition, analyses of hydrographic data and weather reports suggest that in winter, upwelling in the southern Brazil continental shelf is restricted to the shelf break (Lima et al., 1996). The CSAT distribution pattern over the shelf in winter (Fig. 1b), with maxima originated in the Plata estuary, combined with the rather tight CSAT–S relation (Fig. 3) and the prevailing downwelling winds (Figs. 1b) strongly suggest that the CSAT signal at regional scale is primarily associated with the Plata outflow and not to coastal upwelling.

In contrast with the winter situation, in summer upwelling favorable (northeasterly) winds prevail over most of the shelf. Therefore, wind-induced upwelling leads to increased productivity in the South Brazil Bight (e.g., Matsuura, 1996) and off Cape Santa Marta Grande (Odebrecht and Djurfeldt, 1996). Inspection of the CSAT summer distributions (not shown) reveals that at and north of Cape Santa Marta, there are frequent blooms probably associated to wind-induced upwelling. The high CSAT observations in the South Brazil Bight in February 1998 (Fig. 6a) are therefore associated with local upwelling events and not with Plata-derived waters. Upwelling off Cape Santa Marta and the South Brazil Bight are well-known events. Similarly, it is possible that the CSAT increase observed south of the estuary in October–March (Fig. 4a) is due to a combination of local

upwelling and southward advection of Plata-derived waters. However, the summer observation of relatively low *in-situ* surface chl-*a* during periods of reduced Plata influence at 38°S (Carreto et al., 1995, their Figs. 3g–h and 8g–h) suggests that high CSAT observations at that location are mostly associated with southward penetrations of Plata-derived low salinity waters.

5.2. Interannual variability

The northeastward penetration of low salinity water during the EN event of 1998 (~900 km, Fig. 6a), when the Plata outflow exceeded 70,000 $m^3 s^{-1}$ (Figs. 5 and 6d), was less intense than in the winters of 2000–2003, which followed periods of significantly lower outflow (20,000–30,000 $m^3 s^{-1}$). The 1998 event is associated with the fourth largest monthly mean Plata outflow (71,700 $m^3 s^{-1}$), recorded in April 1998, and was only exceeded in May–August during the intense 1983 EN. Piola et al. (2005) have shown that the same anomalous wind patterns that lead to southward advection of water vapor into the Plata basin and increased river outflows during intense EN events also lead to weaker southwesterlies or wind reversals in the coastal region. The less pronounced northward plume penetration in winter 1998 is therefore associated with weak along-shore winds observed throughout the southern Brazil shelf (Fig. 5b), suggesting that the river discharge plays a secondary role in modulating the northward plume extension. In agreement with the recent results of Piola et al. (2005) and Gonzalez-Silvera et al. (2006), our data also show that northernmost plume penetrations, observed during the austral winters of 2000 through 2003, are associated with more intense northeastward along-shore wind stress which extends throughout most of the shelf (Fig. 6b and c). The role of the along-shore wind stress is further illustrated by comparing the winter of 2002 and 2003, which showed very similar plume durations and northward extents (Fig. 6a). Though the wind stress is similar during June of 2002 and 2003 (~0.03 Pa), the Plata outflow was above average (35,000 $m^3 s^{-1}$) in 2002 and below average (18,000 $m^3 s^{-1}$) in 2003.

The weakest northeastward plume penetration in winter (~650 km) was observed in July–August 2004. At that time the wind stress space and time distributions present an anomalous pattern, with weak northeasterly wind stress only apparent south of 32°S (Fig. 6b). For instance at CP τ_y was virtually zero in the winter of 2004 (Fig. 5b). Except for a brief wind reversal observed in April 2004, the northern part of the domain experienced negative (southwestward) τ_y from October 2003 to March 2005 (Figs. 5b and 6b). The lack of wind reversal in the winter of 2004, combined with low Plata outflow from January to October (Fig. 5c), led to the reduced northward penetration of the Plata plume.

The northeastward plume penetration in winter 2003 to about 1200 km from the estuary, and its southwestward retreat to about 600 km in early 2004 (Fig. 6a) are in excellent agreement with the locations of the low surface salinity waters observed during our *in-situ* surveys (e.g. Möller et al., this issue, their Figs. 3b and 7b). This retreat is associated with the change in along-shore wind stress at SP from 0.05 Pa during May–August 2003 to −0.46 Pa in December 2003–January 2004 (Fig. 5b).

Climatological surface salinity distributions show that the southward extension of Plata-derived waters does not present large seasonal variations, as observed north of the estuary (e.g. Piola et al., 2000, their Fig. 3; Lucas et al., 2005, their Fig. 6). As pointed out above, the seasonal CSAT cycle at SP is weaker than at CP and NP. Historical salinity and nutrient data also suggest southward penetrations of Plata waters to the latitude of Mar del Plata, located at 38°S, or about −360 km in along-shore coordinates (e.g. Carreto, 1969; Negri et al., 1992; Carreto et al., 1995). Near-surface salinity data collected between 1984 and 2000 suggest that the extension of low salinity Plata waters beyond Mar del Plata is not frequent. During that period of time only one event was observed in austral fall 1998 ($S<30$, Lucas et al., 2000). South of the estuary the 1998 large outflow event is also evident in the CSAT variability along line AB (Fig. 6a). In agreement with our CSAT space–time plot (Fig. 6a), a near coastal monthly time series of salinity collected just south of Mar del Plata from February 2000 to February 2001 does not present evidence of Plata-derived waters during that time (Lutz et al., 2006). However, several southward extensions of high CSAT–low salinity water beyond −300 km are apparent between early 2001 and early 2004 (Fig. 6a). Our hydrographic observations collected in February 2004 off Mar del Plata, show a shallow (25 m) low salinity (<29) layer in an inner shelf band, which is derived from the Plata (see Möller et al., this issue). At that time CSAT at SP also presented a moderate peak (>6.5 mg m^{-3}, Fig. 5a) and showed a southward plume penetration to about −400 km (Fig. 6a), though the Plata outflow was close to its mean value. Historical surface salinity data shows that further north, close to the location of SP, Plata-derived low salinity waters are frequently observed in late austral spring and summer (Lucas et al., 2000). These observations are in close agreement with the high CSAT observations at SP (Fig. 5a).

5.3. CSAT, outflow and wind stress correlations

CSAT fluctuations close to the estuary do not show such a clear correlation with τ_y. In austral summer of 2002–2003 the Plata plume, as indicated by $\log(\mathrm{CSAT}) = 0.5$, only retreated southwestward to about 600 km northeast of the estuary (Fig. 6a). Consequently, a relatively large portion of the southern shelf presented high CSAT concentrations. However, during that time southwestward wind stress was strong throughout the continental shelf (Fig. 6c) and river outflow was high since early 2002 ($>30{,}000$ $m^3 s^{-1}$), well above the climatological mean. A similar high outflow event, combined with strong northeasterly winds and higher than averaged CSAT concentrations in the southern part of the domain, is apparent in early 1998 (Fig. 6a). On the other hand, lower than averaged $\log(\mathrm{CSAT})$ (<0.8), associated with very low Plata outflow (12,000 $m^3 s^{-1}$) and relatively strong southwestward wind stress (<-0.03 Pa), are observed within the outer estuary in summer 1999–2000. Southwestward wind stress persisted from September 1999 to March 2000 throughout the shelf (Fig. 6b; see also Gonzalez-Silvera et al., 2006, their Fig. 3a). The event may have caused anomalously high near coastal salinity (>34) observed off Uruguay in late January 2000 (Münchow and Framiñan, 2001) and the rare observation of abundant tropical and subtropical species of plankton and fish reaching the estuary, also associated with high salinities (>34) in March 2000 (Mianzan et al., 2001). Interestingly, however, though the wind stress is negative (southwestward) throughout the southern shelf (Fig. 6b), the plume does not extend anomalously southward during the event (Fig. 6a), probably due to the low river outflow.

The ratio of interannual to monthly CSAT standard deviations, estimated for the period 1998–2003, is highest over the region adjacent to and offshore from the outer Plata estuary (Saraceno et al., 2005). The analysis of 8 years of CSAT data shows a spectral peak at interannual time scales (4 years), with highest variability concentrated in a relatively small area just offshore from the estuary (Garcia and Garcia, this issue, their Figs. 5c and 6c). Given that the Plata outflow presents significant variability at interannual time scales (~3.6 years, Garcia and Garcia, this issue) the interannual CSAT variations observed close to the estuary may be associated with the large fluctuations of the river outflow. Thus,

all these observations suggest that the river outflow plays a significant role in the plume development close to the estuary.

To assess to what extent changes in Plata outflow and along-shore wind stress might influence the variations in CSAT distribution we have calculated the correlation coefficients (r) based on the monthly mean time series. Since there might be a delay in CSAT response to changes in river outflow, the calculation was also carried out lagging CSAT in 1 month steps up to +4 months. The procedure was repeated for log(CSAT) with no significant changes in the results. To remove the seasonal signal the correlations were also calculated for CSAT and outflow anomalies around the record-length monthly means. The distribution of r estimated for river outflow anomalies vs. CSAT anomalies at each 9 km × 9 km pixel is presented in Fig. 7a. The r distribution is virtually identical to the one derived from outflow vs. CSAT (not shown), indicating that most of the CSAT variability correlated with river outflow is non-seasonal. The highest correlations were found at 2 month lag, only in the near coastal area, south of the estuary, we found significant correlations at lag zero (not shown), which are not apparent at lag 2. The highest 2-month lagged correlations ($r>0.5$) are limited to the mid-shelf region off the Plata estuary, this is also the area where correlations are significantly different from zero at the 95% confidence level (Fig. 7a). The level of significance is determined considering that observations are independent at 6-month intervals, which is the autocorrelation scale of the Plata outflow. The region of high correlation between CSAT anomalies and river outflow anomalies also matches the location of high CSAT variance and amplitude at interannual time scales (Saraceno et al., 2005; Garcia and Garcia, this issue). These results confirm that variations of the Plata outflow are a significant source of interannual CSAT (and presumably S) variability in the mid-shelf region just offshore from the outer estuary. The results are also in agreement with the limited northward penetration of low salinity waters observed during high Plata outflow events, such as 1998, associated with the more persistent northeasterly winds observed at interannual time scales, which oppose to the development of the coastal current and to the northeastward spreading of low salinity waters (Piola et al., 2005). Another region of high outflow–CSAT correlation is apparent in the southern South Brazil Bight (~26°S, Fig. 7a). Given the distant location from the estuary and its isolation, it is difficult to attribute a physical interpretation to the high correlation in this region.

Significant CSAT–τ_y correlations (Fig. 7b) extend northeastward along the continental shelf, as suggested by the along-shore space–time diagrams of Figs. 6a and b. Monthly wind stress observations are considered independent at 2-month time scale, which is the wind stress autocorrelation scale. Significant CSAT-τ_y correlations were found with lag zero. Southeast of the estuary, enhanced northeastward (southwestward) wind stress leads to the along-shore development (retraction) of the Plata plume, and therefore to low (high) CSAT. This explains the region of significant negative correlations apparent southeast of the estuary (Fig. 7b). CSAT and τ_y anomalies around the record-length monthly means are also positively correlated over the shelf, but, since the time series is too short to quantitatively depict interannual variability, significant correlations are only observed over small areas (not shown). The later result demonstrates the strong impact of the along-shore wind stress on the variability of the coastal current at seasonal time scale. CSAT in the southern Brazil continental shelf is also positively correlated with cross-shore wind stress (not shown). South of 32°S CSAT–τ_y correlations in the inner shelf (depths <50 m) are higher than CSAT–τ_x correlations, while the opposite occurs in the outer shelf. North of 32°S the transition occurs close to the 100 m isobath. Numerical simulations of a river plume in the southern hemisphere, also show a northward plume development which expands offshore when forced by offshore wind stress (Palma and Sitz, 2005). The simulation presents a cross-shore circulation cell in Ekman-type momentum balance, which enhances the cross-shore salinity gradient and, through the baroclinic pressure gradient, also enhances the along-shore flow within the low salinity plume (Palma and Sitz, 2005). This suggests that, in the outer shelf, northeastward flow in the Ekman layer, induced by offshore wind

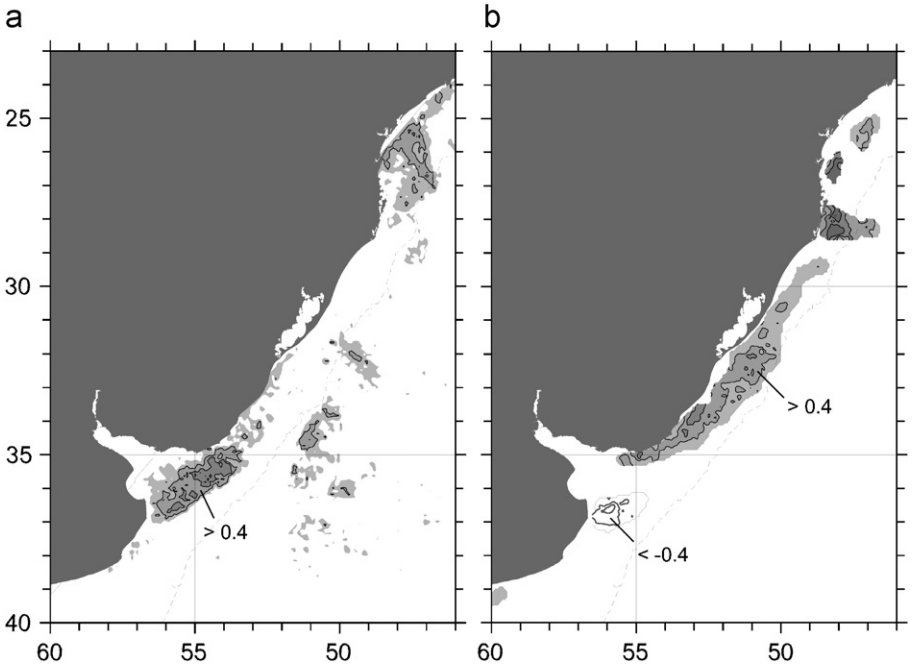

Fig. 7. Correlation coefficient (r) between (a) monthly Plata outflow anomaly and CSAT anomaly (lag+2 months) and (b) between CSAT and along-shore wind stress (zero lag) for the period 1998–2005. Contours are shown only where the correlation is significantly different from zero at 95% confidence. Contour interval is 0.1.

stress, also contributes to the northward extension of the Plata plume. Similarly, the positive CSAT–τ_x correlations suggest that on-shore wind stress acts to retract the plume.

5.4. The rate of CSAT along-shore displacements

The log (CSAT) space–time distribution along line AB (Fig. 6a) suggests that the northeastward plume extension varies from year to year and also that along-shore CSAT displacements occur at variable rates, as indicated by the V_{CSAT} standard deviations around the record-length monthly means (Fig. 4e). The data show that the plume extends northward at about 100 km/month from April to July and retreats at 100–150 km/month from September to February, though it presents a more variable behavior in December. Numerical simulations of the Plata plume forced by 25,000 $m^3 s^{-1}$ outflow and $\sim 10^{-1}$ Pa northeastward wind stress present significantly higher along-shore penetration speeds (0.3 $m s^{-1}$ or 778 km/month, Pimenta et al., 2005). The discrepancy might arise because the model was forced with constant and uniformly distributed winds, indeed unrealistic at seasonal time scales, but perhaps representative of short-term wind episodes, while the CSAT observations represent monthly mean plume variations. The CSAT rate of displacement can be compared with along shelf changes in surface salinity as observed during the Nicop–Laplata surveys, which were carried out close to the peak of the plume expansion in late August 2003 and the following retraction in early February 2004. During this period the mean along-shore wind stress at NP was −0.06 Pa. In Austral winter 2003 the 30 isohaline extended northeastward along the shelf to about 28°50′S and in the following summer it was located at 35°S (see Figs. 3b and 7b, Möller et al., this issue). In 165 days the isohaline displaced southwestward 860 km, i.e. at a rate of 0.06 $m s^{-1}$ or 156 km/month. The above displacement is in close agreement with the mean retraction of the 0.5 log (CSAT) isopleth during the same period (130 km/month = 0.05 $m s^{-1}$).

Given that our basic assumption is that CSAT can be considered a passive tracer, it is also useful to discuss the relative importance of horizontal advection in causing the variability in CSAT distributions. There are few current observations available in the southern Brazil continental shelf. Three surface drifters deployed in late April and May 1993 between 33 and 28°S and reaching past 25°S, showed a persistent northeastward flow in the upper layer at a speed of 0.11 ± 0.06 $m s^{-1}$ (Souza and Robinson, 2004). Near-surface (15 m) observations collected from early March to late May 1997 at a mooring located near 32°40′S, close to the 50 m isobath, reveal a northeastward mean flow of $\sim 0.16 \pm 0.26$ $m s^{-1}$ (Zavialov et al., 2002). The significantly lower mean flow observed after that period ($\sim 0.06 \pm 0.31$ $m s^{-1}$) is presumably associated with the presence of the low salinity upper layer, which decouples the 15 m currents from direct wind effects (Zavialov et al., 2002).

The variability of the upper layer flow is further investigated based on all surface drifters available in the region between the coast and the winter location of 33.5, and from 34°S to 25°S. This latitude range includes the region of largest CSAT (Fig. 6a) and salinity (Fig. 1) seasonal variability. The drifter 6 hourly velocity data is from Pazan and Niiler (2004). In the period 1993–2004 there are 30 drifters that fit the selection criteria, totaling 2530 velocity estimates (or about 630 drifter days). The monthly mean along-shore surface velocities present the expected seasonal pattern based on the along-shore wind stress variability: positive (northeastward) flow from March through July and negative (southwestward) flow from August through February (Fig. 4e). Though the drifter-derived monthly means are remarkably stable (Fig. 4e), we should bear in mind that the space–time distribution of the observations is non-uniform. Northward velocities peak in July (~ 0.26 $m s^{-1}$ or 685 km/month) and southward velocities in October (-0.12 $m s^{-1}$ or −309 km/month). Thus, though the flow direction matches the CSAT and salinity plume propagation directions, the surface currents are larger than the plume-spreading rate by a factor of 2–3 (Fig. 4e). The velocity mismatch must be a consequence of significant contributions from turbulent mixing and/or vertical and cross-shore advection to the local salinity balance, which would act to decrease the spreading rate of the salinity field.

During the Nicop–Laplata experiments at 30°S we observed a salinity variation of 5.5 in ~164 days, leading to a local rate of change ($\partial S/\partial t$) of $\sim 4 \times 10^{-7}$ s^{-1}. The local rate of change is about 25% of our estimates of along-shore salinity advection derived from the drifter velocities combined with the *in-situ* salinity data: $v\ \partial S/\partial y = 0.15$ $m s^{-1} \times 1.1 \times 10^{-5}$ $m^{-1} \approx 1.6 \times 10^{-6}$ s^{-1}. The drifter-derived cross-shore velocities are generally small compared with the along-shore velocities, and offshore flow ($\sim 2 \times 10^{-2}$ $m s^{-1}$) is only observed from May to July. Nevertheless, combined with the large cross-shore salinity gradient estimated from the Nicop–Laplata surveys ($\partial S/\partial x \sim 4 \times 10^{-4}$ m^{-1}), the positive cross-shore velocity can lead to significant offshore advection ($u\ \partial S/\partial x \sim 2 \times 10^{-6}$ s^{-1}) at the plume front. The salinity balance of the simplified plume model of Palma and Sitz (2005) shows that when forced by southerly winds the downstream (northward) advection in the inner shelf is balanced by comparable contributions from horizontal and vertical diffusion. The model also shows that offshore advection is significant at the location of the salinity front, where it is balanced by vertical diffusion and along-shore (negative) advection, but not near shore, within the low salinity waters (Palma and Sitz, 2005, their Fig. 7). The negative along-shore advection in the simulation arises from the northward plume spreading, which causes negative along-shore salinity gradients (e.g. a southward salinity increase) at the outer edge of the plume front. Since the model balance is calculated for a relatively short time (30 days), it predicts negligible local salinity changes ($\partial S/\partial t$). Though from this analysis we cannot draw definite conclusions on which mechanisms balance the along-shore salinity advection, the combined satellite, *in situ* and drifter data suggest that the salinity changes observed northeast of the estuary at seasonal time scales are primarily associated to changes in the along-shore advection. These findings appear to be in overall agreement with the salinity balance derived from numerical simulations (Palma and Sitz, 2005).

Model simulations forced by upwelling (northeasterly) winds, characteristic of the spring–summer seasons, applied on well-developed coastal plumes show rapid (5–10 days) offshore displacements of low salinity waters (Pimenta et al., 2005). The reduced difference between plume spreading and flow velocity during the retraction phase (Fig. 4e) suggests that advection plays a more significant role in the southwestward retreat of low salinity waters in austral spring and early summer. The strong northeasterly winds extending throughout the domain in spring–summer (Fig. 4a–c) may be responsible for the strong southward surface flow near the coast (Fig. 4e). Offshore advection of low salinity waters within the Ekman layer associated with the strong northeasterlies may explain the rapid plume "retreat" suggested by the CSAT data (Fig. 4e, see also Palma and Sitz, 2005). Historical salinity data (Fig. 1a) and the Nicop–Laplata surveys present the offshore spreading of the low salinity waters south of the estuary (see Fig. 1 Möller et al., this issue, their Fig. 7b). Offshore advection of coastal waters in summer also widens the CSAT plume south of the estuary (e.g. Fig. 1a and Garcia and Garcia, this issue, their Fig. 3d). The offshore flowing low salinity waters mix with the swift and comparatively large Brazil Current near the shelf break leading to the frequent austral summer observation of low salinity surface waters within the Brazil Current and further downstream

within the Brazil/Malvinas Confluence (e.g. Gordon, 1989; Provost et al., 1996).

6. Conclusions

The analysis presented here reveals that satellite-derived surface chl-*a* concentrations estimated by the OC4v4 SeaWiFS retrieval algorithm can be used as an indicator of low salinity surface waters derived from the outflow of the Plata river as they spread on the continental shelf. Simultaneous *in-situ* salinity observations show that the salinity transition from Plata plume to shelf waters occurs within the 28.5–32.5 range and that CSAT concentrations higher than 5 mg m^{-3} are associated with surface waters of salinity lower than 31. In austral winter CSAT maxima typically extend northeastward from the Plata estuary beyond 30°S. In summer the high CSAT waters occupy most of the continental shelf width east and southeast of the estuary. The average summer southwestward near-shore plume penetration is 37.5°S and the northeastward extent along the shelf is limited to about 32°S. The seasonal CSAT variations are primarily controlled by the along-shore wind stress. Winter downwelling winds generate on-shore Ekman transport; increase the cross-shore pressure gradient and favor the northeastward flow which spreads the high CSAT waters. These variations closely resemble the seasonal migrations of the surface salinity derived from historical hydrographic data. The CSAT data also present large interannual variations, with winter-like northernmost penetrations associated with most intense and persistent northeastward wind stress, which prevail over the entire shelf (e.g. winter of 2000). The plume response to the rather large river outflow fluctuations observed at interannual time scales is moderate, except near the estuary mouth, where CSAT variations lag outflow variations by 2 months, suggesting that in this region the outflow variability is more important than the wind effect. The plume spreads along-shore at a rate of about 100–150 km/month. Salinity changes at seasonal time scale are primarily controlled by upper layer flow and wind stress reversals in the along-shore direction. The development of a coastal plume southwest of the estuary mouth during the summer, when northeasterly winds prevail, is limited, suggesting that low salinity waters are exported to the outer shelf, where it is presumably lost within the intense western boundary currents. Only in extraordinary occasions does the low salinity water extend along the coast beyond Mar del Plata (38°S). These results show that CSAT is a useful indicator of the spreading of the Plata-derived low salinity waters along the continental shelf of South America. CSAT may be useful to determine the fate of other large continental discharges into the ocean, though specific CSAT–surface salinity relations at other locations may differ from those found off the Río de la Plata estuary.

Acknowledgements

This research was funded by the Inter-American Institute for Global Change Research (Grants CRN-061 and CRN2076, the IAI is funded by the US National Science Foundation Grant GEO-0452325) and Fundación Antorchas (Grant 13900-13). Additional funding was provided by a Naval International Cooperative Opportunities in Science and Technology Program grant from the US Office of Naval Research. We acknowledge Diretoria de Hidrografia e Navegaçao (Brazil), Servicio de Hidrografía Naval (Argentina) and Servicio de Oceanografía, Hidrografía y Meteorología (Uruguay) for their cooperation in obtaining clearance for carrying out field work within EEZs, and the crews of RV *NOc ANTARES* and *ARA PUERTO DESEADO* and the scientific parties of both cruises for their valuable cooperation at sea. SeaWiFS data are provided by NASA's Goddard Space Flight Center and Orbimage. QuikSCAT data are produced by Remote Sensing Systems and sponsored by the NASA Ocean Vector Winds Science Team and ERS data were obtained from CERSAT, IFREMER, Plouzané (France). We thank R. Guerrero for useful discussions on the oceanography of the Plata estuary, for suggesting key references and providing unpublished data; and M. Acha, C. Garcia and S. Signorini, for providing helpful comments on an earlier draft of this manuscript.

References

Acha, E.M., Mianzan, H., Guerrero, R.A., Carreto, J.I., Giberto, D., Montoya, N., Carignan, M.O., An overview of physical and ecological processes in the Rio de la Plata estuary. Continental Shelf Research, this issue, doi:10.1016/j.csr.2007.01.031.

Armstrong, R.A., Gilbes, F., Guerrero, R., Lasta, C., Benavidez, H., Mianzan, H., 2004. Validation of SeaWiFS-derived chlorophyll for the Rio de la Plata Estuary and adjacent waters. International Journal of Remote Sensing 25 (7–8), 1501–1505.

Binding, C.E., Bowers, D.G., 2003. Measuring the salinity of the Clyde Sea from remotely sensed ocean color. Estuarine, Coastal and Shelf Science 57, 605–611.

Borús, J., Uriburu Quirno, M., Calvo, D., 2006. Evaluación de caudales diarios descargados por grandes ríos del sistema del Plata al estuario del Río de la Plata. Alerta Hidrológico-Instituto Nacional del Agua y el Ambiente, Ezeiza, Argentina.

Campos, E.J.D., Lentini, C.A.D., Miller, J.L., Piola, A.R., 1999. Interannual variability of the sea surface temperature in the South Brazil Bight. Geophysical Research Letters 26, 2061–2064.

Carreto, J.I., 1969. Variaciones de la biomasa fitoplanctónica en aguas costeras de Mar del Plata. Comisión Asesora Regional de Pesca para el Atlántico Sudoccidental, Documentos Ocasionales 11, 14pp.

Carreto, J.I., Negri, R.M., Benavides, H.R., 1986. Algunas características del florecimiento del fitoplancton en el frente del Río de la Plata. I: Los sistemas nutritivos. Revista de Investigación y Desarrollo Pesquero 5, 7–29.

Carreto, J.I., Lutz, V.A., Carignan, M.O., Colleoni, A.D.C., Marcos, S.G.D., 1995. Hydrograph and chlorophyll-*a* in a transect from the coast to the shelf-break in the Argentinean Sea. Continental Shelf Research 15, 315–336.

Ciotti, A.M., Odebrecht, C., Fillmann, G., Möller Jr., O.O., 1995. Freshwater outflow and subtropical convergence influence on phytoplankton biomass on the southern Brazilian continental shelf. Continental Shelf Research 15, 1737–1756.

Depetris, P.J., Kempe, S., Latif, M., Mook, W.G., 1996. ENSO controlled flooding in the Paraná River (1904–1991). Naturwissenschaften 83, 127–129.

Eichler, P.P.B., Sen Gupta, B.K., Beck Eichler, B., Campos, E.J.D., Foraminiferal diversity trends in the sediments of the Brazilian continental shelf between 27°S and 30°S. Continental Shelf Research, this issue, doi:10.1016/j.csr.2007.10.012.

Emilson, I., 1961. The shelf and coastal waters off southern Brazil. Boletim do Instituto Oceanográfico 11 (2), 101–112.

Framiñan, M.B., Etala, M.P., Acha, E.M., Guerrero, R.A., Lasta, C.A., Brown, O.B., 1999. Physical characteristics and processes of the Río de la Plata Estuary. In: Perillo, G.M., Piccolo, M.C., Pino-Quivira, M. (Eds.), Estuaries of South America: Their Geomorphology and Dynamics. Springer, New York, pp. 161–194 (Chapter 8).

Garcia, C.A.E., Garcia, V.M.T. Variability of chlorophyll-*a* from ocean color images in the La Plata continental shelf region. Continental Shelf Research, this issue, doi:10.1016/j.csr.2007.08.010.

Garcia, C.A.E., Garcia, V.M.T., McClain, C.R., 2005. Evaluation of SeaWiFS chlorophyll algorithms in the Southwestern Atlantic and Southern Oceans. Reomote Sensing of Environment 95, 125–137.

Garcia, V.M.T., Signorini, S., Garcia, C.A.E., McClain, C.R., 2006. Empirical and semi-analytical chlorophyll algorithms in the southwestern Atlantic coastal region (25–40°S and 60–45°W). International Journal of Remote Sensing 27 (8), 1539–1562.

Garvine, R.W., 1999. Penetration of buoyant coastal discharge onto the continental shelf: a numerical model experiment. Journal of Physical Oceanography 29, 1892–1909.

Gonzalez-Silvera, A., Santamaria-del-Angel, E., Garcia, V.M.T., Garcia, C.A.E., Millán-Nuñez, R., Muller-Karger, F., 2004. Biogeographical regions of the tropical and subtropical Atlantic Ocean off South America: classification based on pigment (CZCS) and chlorophyll-*a* (SeaWiFS) variability. Continental Shelf Research 24, 983–1000.

Gonzalez-Silvera, A., Santamaria-del-Angel, E., Millán-Núñez, R., 2006. Spatial and temporal variability of the Brazil–Malvinas Confluence and the La Plata Plume as seen by SeaWiFS and AVHRR imagery. Journal of Geophysical Research 111, C06010.

Gordon, A.L., 1989. Brazil–Malvinas confluence—1984. Deep Sea Research Part A 36, 359–384.

Guerrero, R.A., Acha, E.M., Framiñan, M.B., Lasta, C.A., 1997. Physical oceanography of the Río de la Plata Estuary. Continental Shelf Research 17, 727–742.
Hu, C., Carder, K.L., Muller-Karger, F.E., 2000. Atmospheric correction of SeaWiFS imagery: assessment of the use of alternative bands. Applied Optics 39 (21), 3573–3581.
Huret, M., Dadou, I., Dumas, F., Lazure, P., Garçon, V., 2005. Coupling physical and biogeochemical processes in the Río de la Plata plume. Continental Shelf Research 25, 629–653.
International Ocean-Colour Coordinating Group, 2000. Remote sensing of ocean colour in coastal, and other optically-complex waters. In: Sathyendranath, S. (Ed.), Reports of the International Ocean-Colour Coordinating Group, No. 3. IOCCG, Dartmouth, Canada.
Kiladis, G.N., Diaz, H.F., 1989. Global climate anomalies associated with extremes in the Southern Oscillation. Journal of Climate 2, 1069–1090.
Kourafalou, V.H., Oey, L.-Y., Wang, J.D., Lee, T.N., 1996. The fate of river discharge on the continental shelf, 1, modeling the river plume and the inner shelf coastal current. Journal of Geophysical Research 101, 3415–3434.
Lima, I.D., Garcia, C.A., Möller, O.O., 1996. Ocean surface processes on the southern Brazilian shelf: characterization and seasonal variability. Continental Shelf Research 16 (10), 1307–1317.
Lucas, A.J., Guerrero, R.A., Mianzan, M.W., Acha, E.M., Lasta, C.A., 2000. On the coastal oceanographic regimes of the Northern Argentine Continental Shelf Paper presented at the IV Jornadas Nacionales de Ciencias del Mar, Puerto Madryn, Argentina, p. 84.
Lucas, A.J., Guerrero, R.A., Mianzan, M.W., Acha, E.M., Lasta, C.A., 2005. Coastal oceanographic regimes of the Northern Argentine Continental Shelf (34–43°S). Estuarine Coastal and Shelf Science 65, 405–420.
Lutz, V.A., Subramaniam, A., Negri, R.M., Silva, R.I., Carreto, J.I., 2006. Annual variations in bio-optical properties at the 'Estación Permanente de Estudios Ambientales (EPEA)' coastal station, Argentina. Continental Shelf Research 26, 1093–1112.
Matsuura, Y., 1996. A probable cause of recruitment failure of the brazilian sardine (*Sardinella aurita*) population during the 1974/1975 spawning season. South African Journal of Marine Sciences 17, 29–35.
Mechoso, C.R., Perez Iribarren, G., 1992. Streamflow in southeastern South America and the Southern Oscillation. Journal of Climate 5, 1535–1539.
Mianzan, H.W., Acha, E.M., Guerrero, R.A., Ramirez, F.C., Sorarrain, D.R., Simionato, C., Borus, J., 2001. South Brazilian Marine Fauna in the Río de la Plata Estuary Paper presented at the IX COLACMAR, Colombia.
Möller Jr., O.O, Piola, A.R., Freitas, A.C., Campos, E.J.D. The effects of the river discharge and seasonal winds on the shelf off Southeastern South America. Continental Shelf Research, this issue, doi:10.1016/j.csr.2008.03.012.
Muelbert, J.H., Sinque, C., 1996. The distribution of bluefish larvae (*Pomatomus saltatrix*) in the continental shelf of southern Brazil. Marine and Freshwater Research 47, 311–314.
Münchow, A., Framiñan, M.B., 2001. Kinematics of a topographically steered poleward shelf flow off Uruguay Abstract, IAPSO/IABO Joint Assembly, IB01-96, Mar del Plata, Argentina.
Negri, R.M., Carreto, J.I., Benavides, H.R., Akselman, R., Lutz, V.A., 1992. An unusual bloom of *Gyrodinium* cf. *aureolum* in the Argentine sea: community structure and conditioning factors. Journal of Plankton Research 41 (2), 261–269.
Odebrecht, C., Djurfeldt, L., 1996. The role of nearshore mixing on phytoplankton size structure off Cape Santa Marta Grande, southern Brazil (Spring 1989). Archive of Fisheries and Marine Research 43 (3), 217–230.
Palma, E.D., Sitz, L.E., 2005. Dinámica de gran escala de plumas poco densas. In: Larreteguy, A. (Ed.), Mecánica Computacional 24. Asociación Argentina de Mecánica Computacional, Buenos Aires, pp. 3303–3320.
Patt, F.S., Barnes, R.A., Eplee Jr., R.E., Franz, B.A., Robinson, W.D., Feldman, G.C., Bailey, S.W., Gales, J., Werdell, P.J., Wang, M., Frouin, R., Stumpf, R.P., Arnone, R.A., Gould Jr., R.W., Martinolich, P.M., Ransibrahmanakul, V., O'Reilly, J.E., Yoder, J.A., 2003. Algorithm updates for the fourth SeaWiFS data reprocessing. In: Hooker, S.B., Firestone, E.R. (Eds.), NASA Technical Memorandum 2003-206892, vol. 22. NASA Goddard Space Flight Center, Greenbelt, MD, 74pp.
Pazan, S.E., Niiler, P., 2004. New global drifter data set available. Eos 85 (2), 17 available at http://www.agu.org/eos_elec/000440e.shtml.
Pimenta, F.M., Campos, E.J.D., Miller, J.L., Piola, A.R., 2005. Numerical study of the river discharge and wind effects over the Plata River plume intrusion the southeastern South American Shelf. Brazilian Journal of Oceanography 53 (3–4), 129–146.
Piola, A.R., Romero, S.I., 2004. Analysis of space–time variability of the Plata River Plume. Gayana 68 (2), 482–486.
Piola, A.R., Campos, E.J.D., Möller Jr., O.O., Charo, M., Martinez, C.M., 2000. Subtropical shelf front off eastern South America. Journal of Geophysical Research 105 (C3), 6566–6578.
Piola, A.R., Matano, R.P., Palma, E.D., Möller Jr., O.O., Campos, E.J.D., 2005. The influence of the Plata River discharge on the western South Atlantic Shelf. Geophysical Research Letters 32, L01603.
Piola, A.R., Möller Jr., O.O., Guerrero, R.A., Campos, E.J.D., Variability of the subtropical shelf front off eastern South America: winter 2003 and summer 2004. Continental Shelf Research, this issue, doi:10.1016/j.csr.2008.03.013.
Provost, C., Garçon, V., Medina Falcon, L., 1996. Hydrographic conditions in the surface layers over the slope-open ocean transition area near the Brazil–Malvinas confluence during austral summer 1990. Continental Shelf Research 16 (2), 215–219.
Ropelewski, C.H., Halpert, S., 1987. Global and regional scale precipitation patterns associated with El Niño/Southern Oscillation. Monthly Weather Review 115, 1606–1626.
Saraceno, M., Provost, C., Piola, A.R., 2005. On the relationship between satellite-retrieved surface temperature fronts and chlorophyll a in the western South Atlantic. Journal of Geophysical Research 110, C11016.
Simionato, C.G., Nuñez, M.N., Engel, M., 2001. The salinity front of the Rio de la Plata—a numerical case study for winter and summer conditions. Geophysical Research Letters 28, 2641–2644.
Souza, R.B., Robinson, I.S., 2004. Lagrangian and satellite observations of the Brazilian Coastal Current. Continental Shelf Research 24, 241–262.
Stevenson, M.R., Dias-Brito, D., Stech, J.L., Kampel, M., 1998. How do cold water biota arrive in a tropical bay near Rio de Janeiro, Brazil? Continental Shelf Research 18 (13), 1595–1612.
Sunyé, P.S., Servain, J., 1998. Effects of seasonal variations in meteorology and oceanography on the Brazilian sardine fishery. Fisheries Oceanography 7, 89–100.
Zavialov, P.O., Möller Jr., O.O., Campos, E.J.D., 2002. First direct measurements of currents on the continental shelf of southern Brazil. Continental Shelf Research 22, 1975–1986.